atmosphere

# Supplementary Material S5

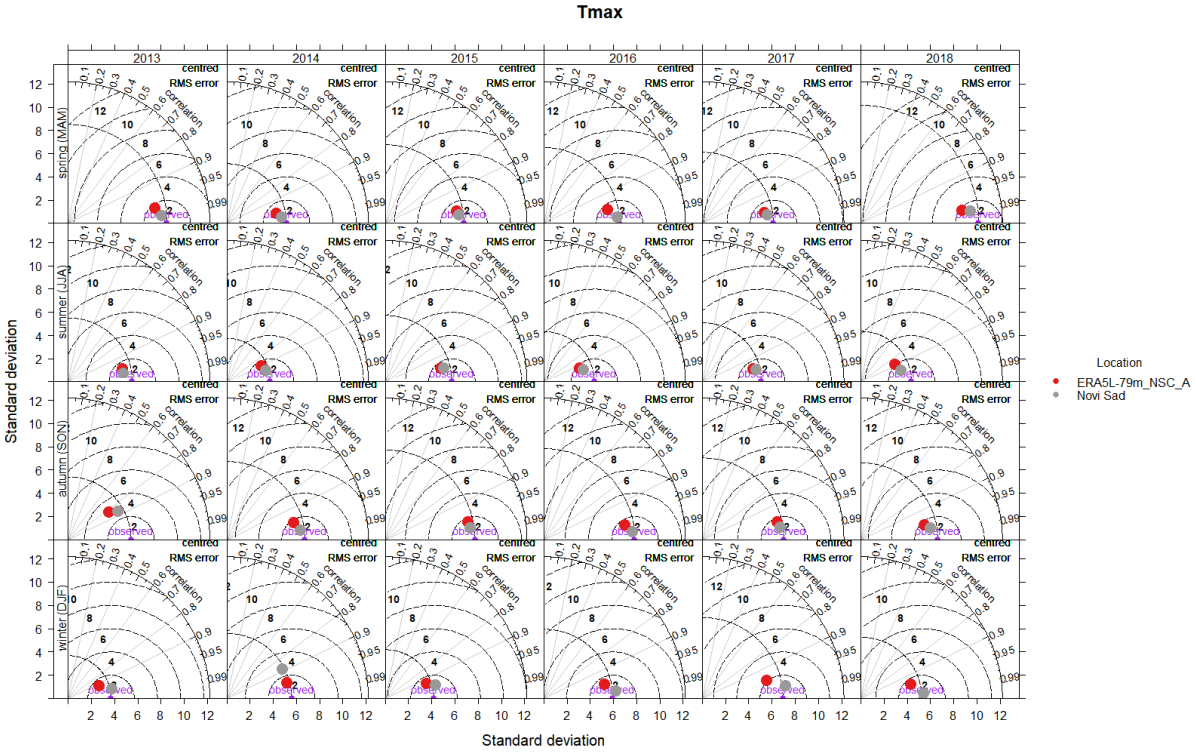


**Figure S5.1** Seasonal Taylor diagram of the $T_{max}$ during the period 2013–2018 observed on 79m_NSC_A AWS in respect to Novi Sad climatological station and ERA5-Land reanalysis for the point closest to 79m_NSC_A.

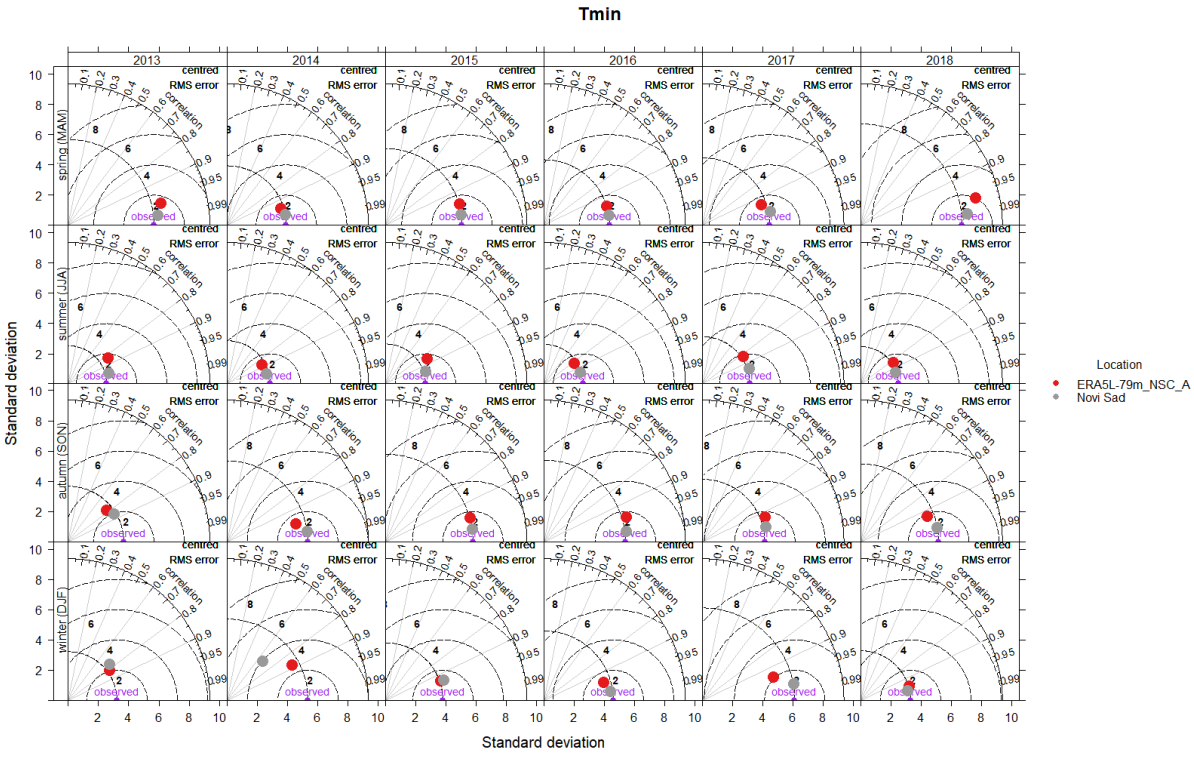


**Figure S5.2** Seasonal Taylor diagram of the $T_{min}$ during the period 2013–2018 observed on 79m_NSC_A AWS in respect to Novi Sad climatological station and ERA5-Land reanalysis for the point closest to 79m_NSC_A.

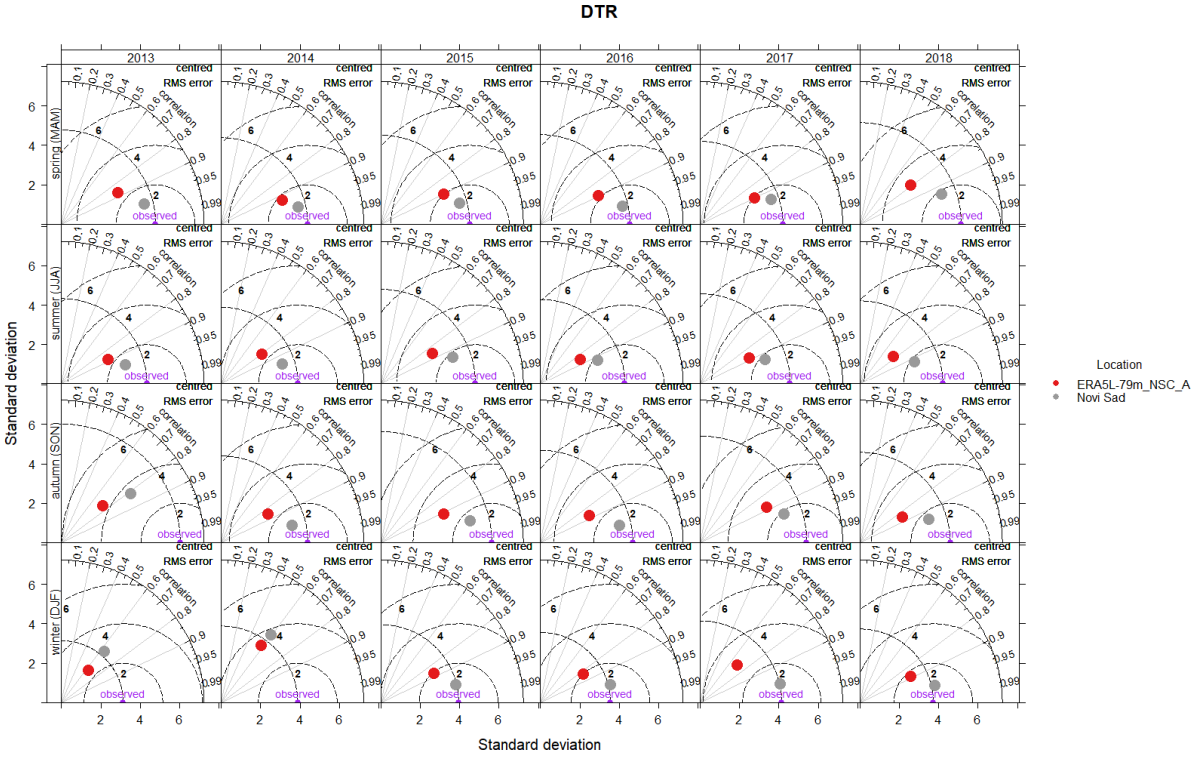


**Figure S5.3** Seasonal Taylor diagram of the DTR during the period 2013–2018 observed on 79m_NSC_A AWS in respect to Novi Sad climatological station and ERA5-Land reanalysis for the point closest to 79m_NSC_A.

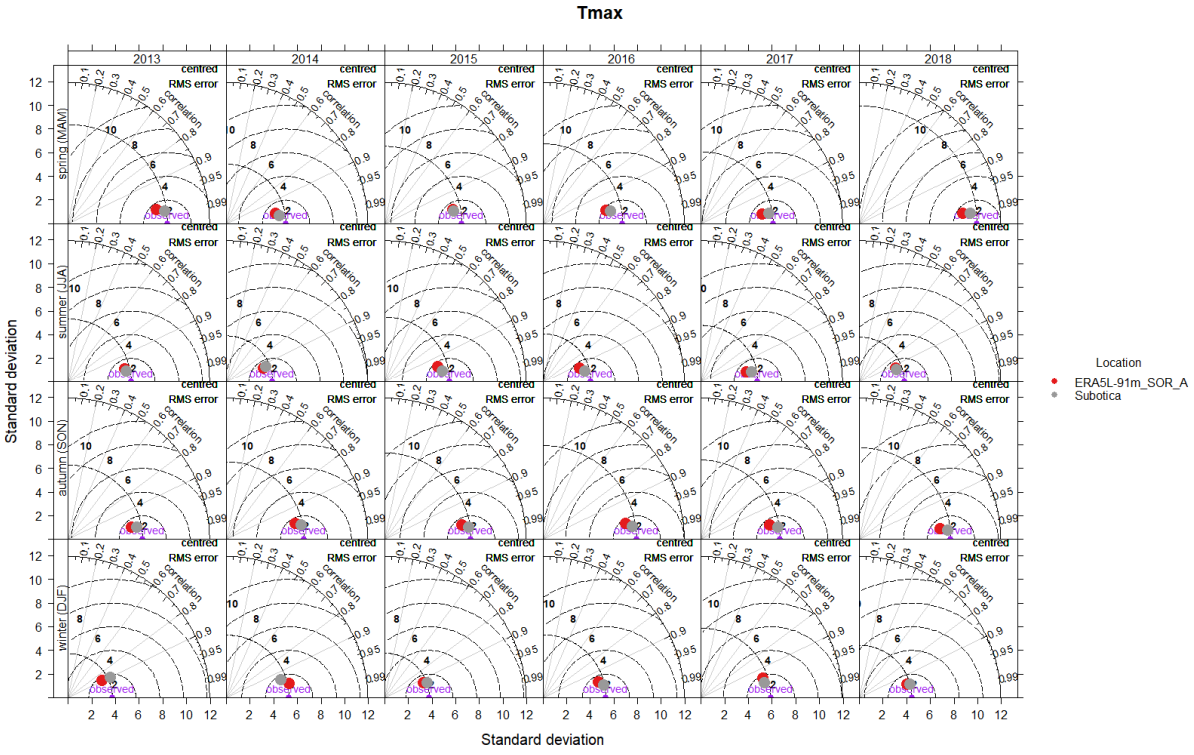


**Figure S5.4** Seasonal Taylor diagram of the $T_{max}$ during the period 2013–2018 observed on 91m_SOR_A AWS in respect to Subotica climatological station and ERA5-Land reanalysis for the point closest to 91m_SOR_A.

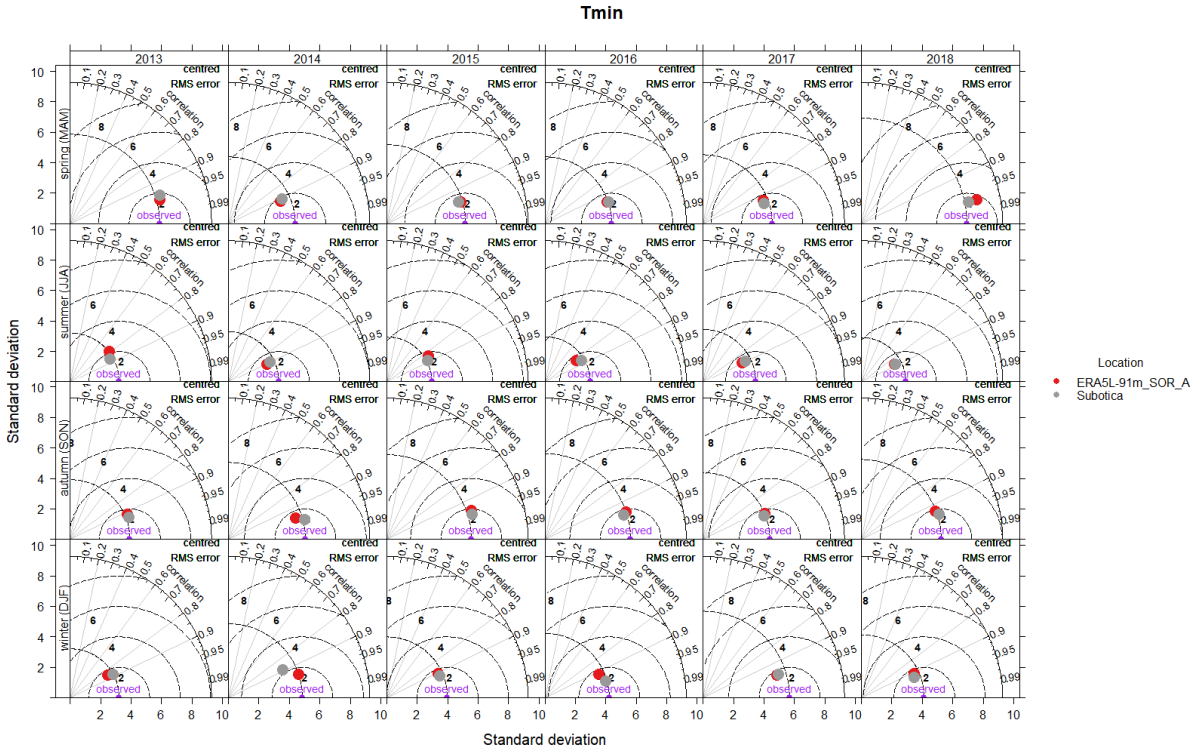


**Figure S5.5** Seasonal Taylor diagram of the $T_{min}$ during the period 2013–2018 observed on 91m_SOR_A AWS in respect to Subotica climatological station and ERA5-Land reanalysis for the point closest to 91m_SOR_A.

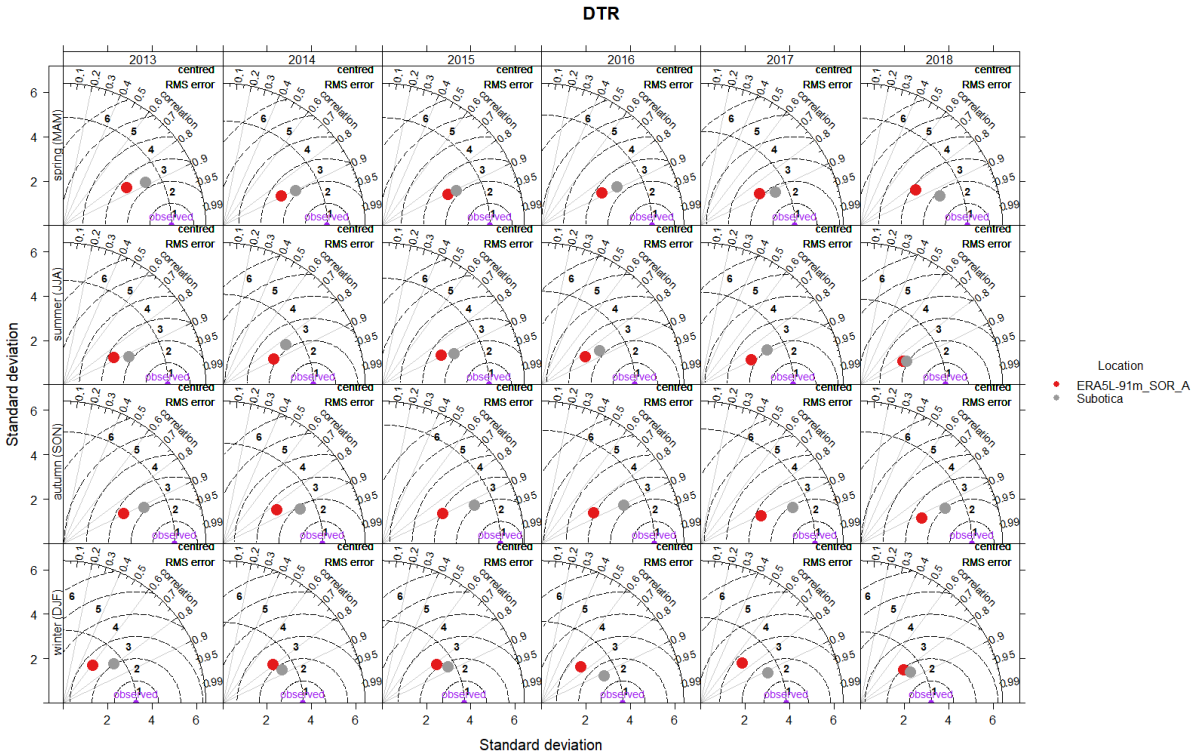

**Figure S5.6** Seasonal Taylor diagram of the DTR during the period 2013–2018 observed on 91m_SOR_A AWS in respect to Subotica climatological station and ERA5-Land reanalysis for the point closest to 91m_SOR_A.

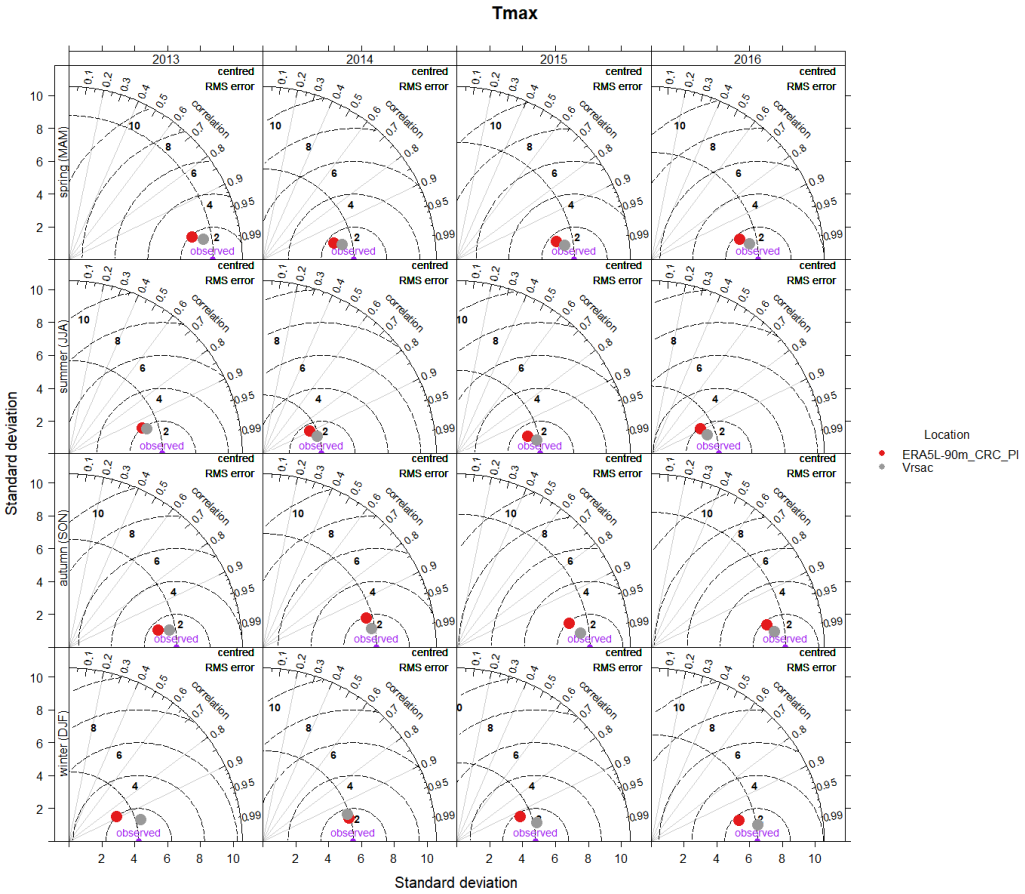


**Figure S5.7** Seasonal Taylor diagram of the $T_{max}$ during the period 2013–2016 observed on 90m_CRC_Pl AWS in respect to Vrsac climatological station and ERA5-Land reanalysis for the point closest to 90m_CRC_Pl.

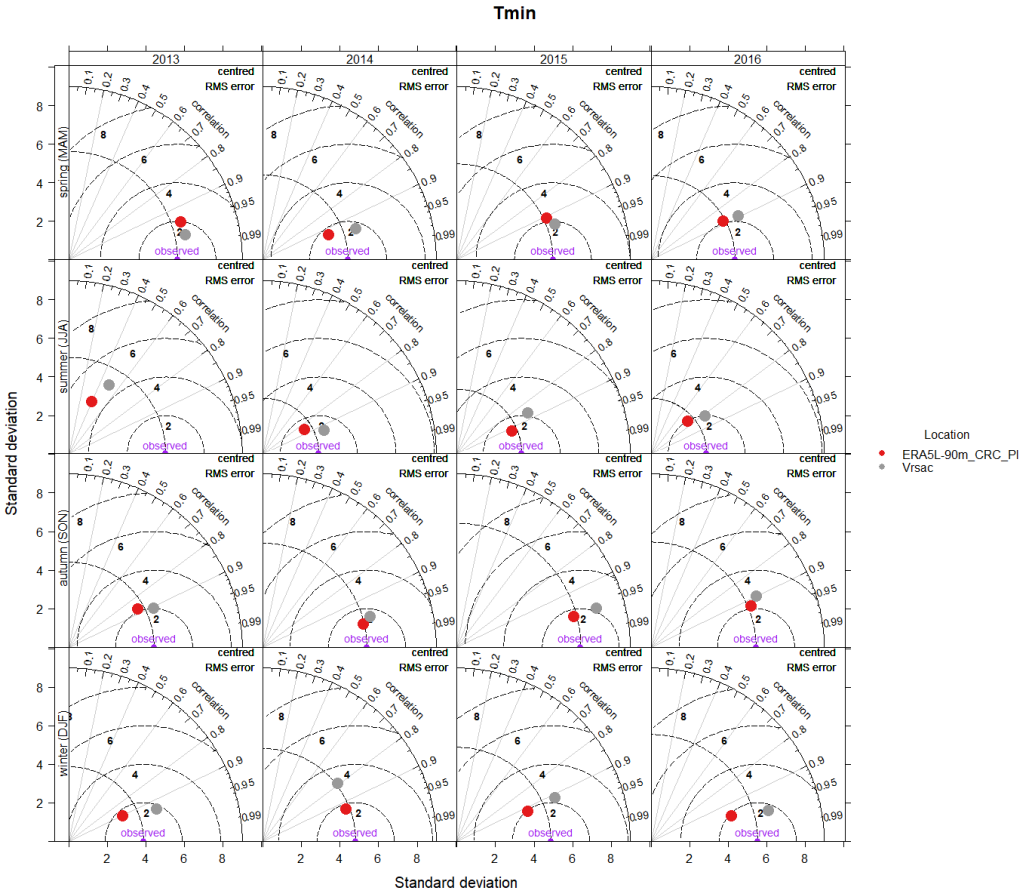


**Figure S5.8** Seasonal Taylor diagram of the $T_{min}$ during the period 2013–2016 observed on 90m_CRC_Pl AWS in respect to Vrsac climatological station and ERA5-Land reanalysis for the point closest to 90m_CRC_Pl.

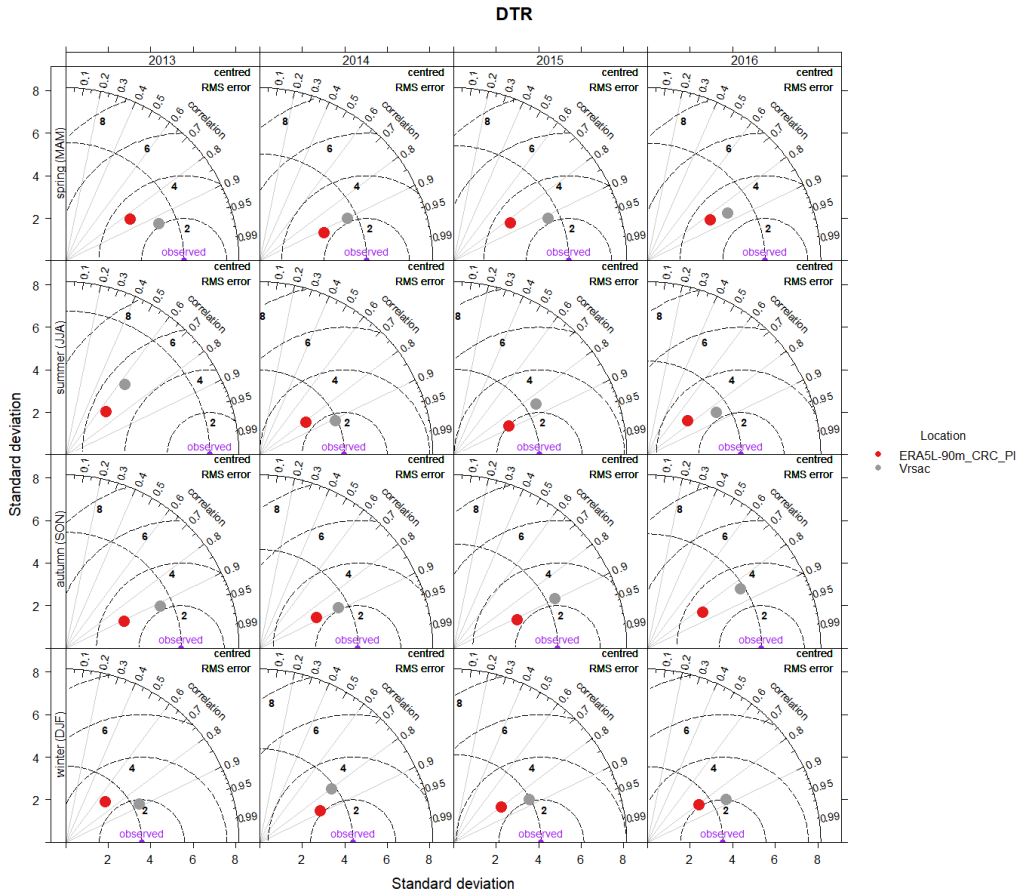

**Figure S5.9** Seasonal Taylor diagram of the DTR during the period 2013–2018 observed on 90m_CRC_Pl AWS in respect to Vrsac climatological station and ERA5-Land reanalysis for the point closest to 90m_CRC_Pl.

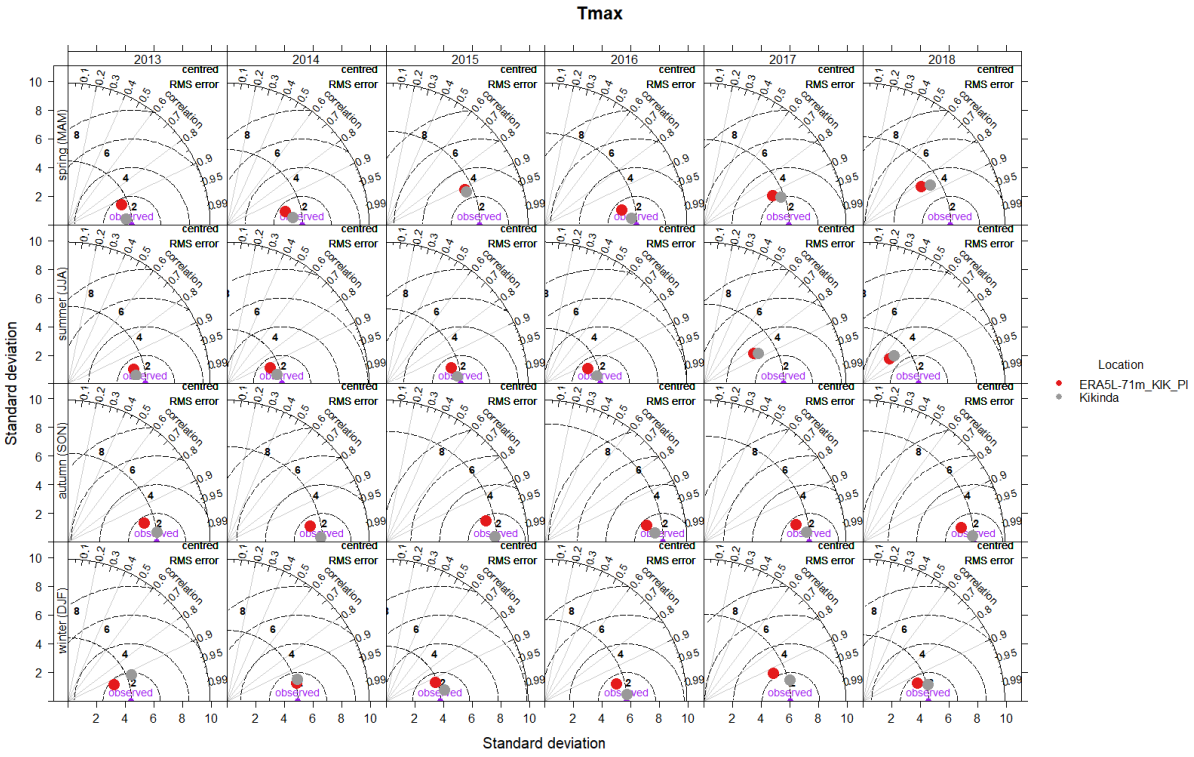


**Figure S5.10** Seasonal Taylor diagram of the $T_{max}$ during the period 2013–2018 observed on 71m_KIK_Pl AWS in respect to Kikinda climatological station and ERA5-Land reanalysis for the point closest to 71m_KIK_Pl.

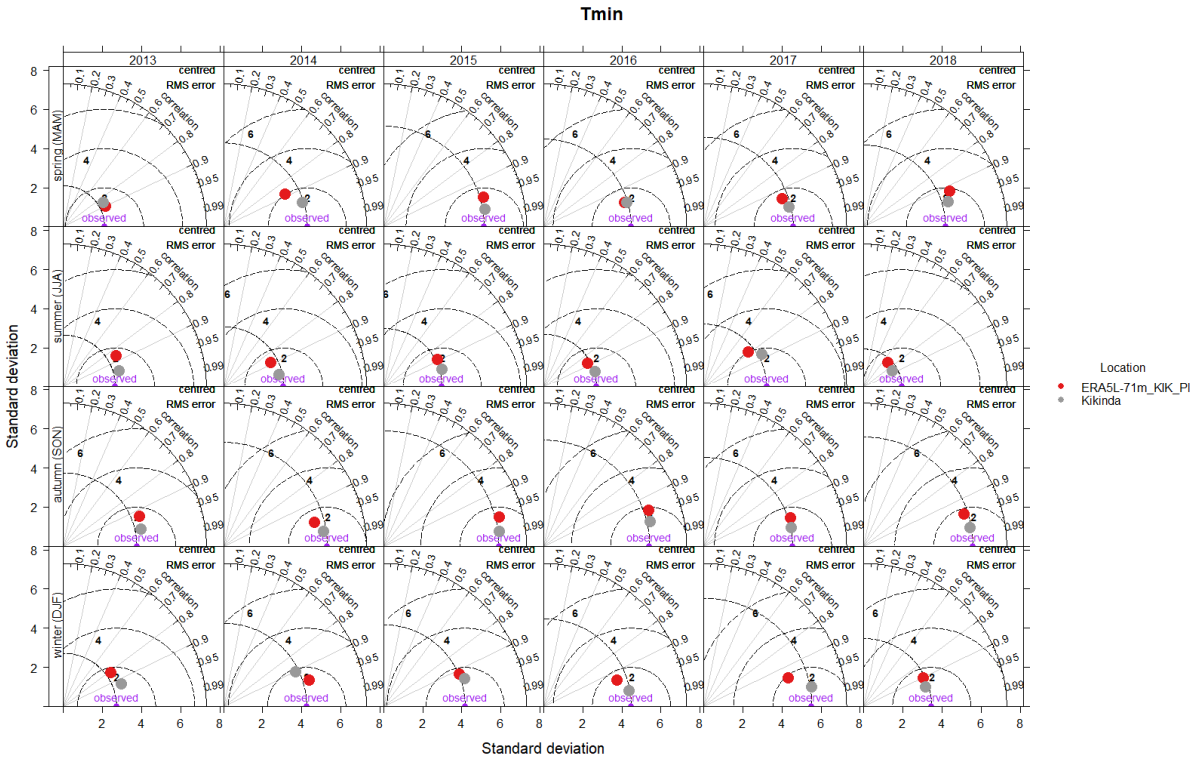


**Figure S5.11** Seasonal Taylor diagram of the $T_{min}$ during the period 2013–2018 observed on 71m_KIK_Pl AWS in respect to Kikinda climatological station and ERA5-Land reanalysis for the point closest to 71m_KIK_Pl.

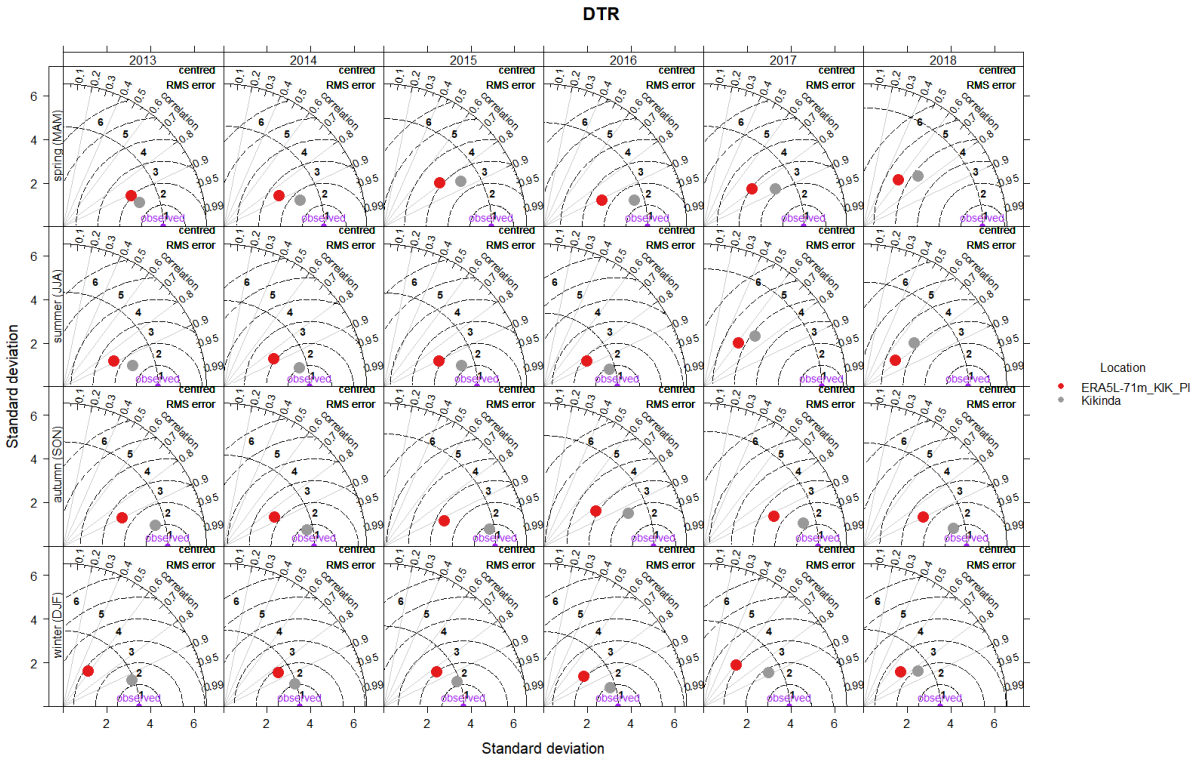

**Figure S5.12** Seasonal Taylor diagram of the DTR during the period 2013–2018 observed on 71m_KIK_Pl AWS in respect to Kikinda climatological station and ERA5-Land reanalysis for the point closest to 71m_KIK_Pl.

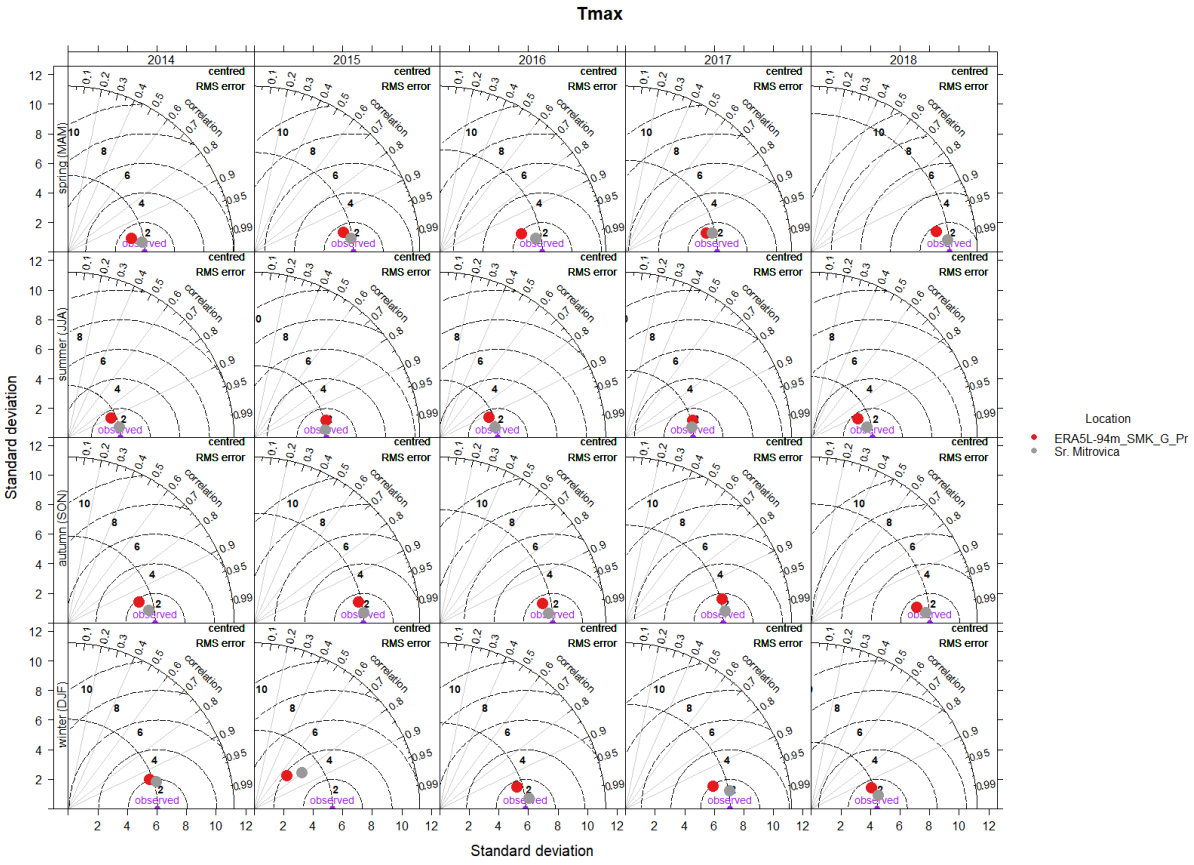


**Figure S5.13** Seasonal Taylor diagram of the $T_{max}$ during the period 2013–2018 observed on 94m_SMK_G_Pr AWS in respect to Sr. Mitrovica climatological station and ERA5-Land reanalysis for the point closest to 94m_SMK_G_Pr.

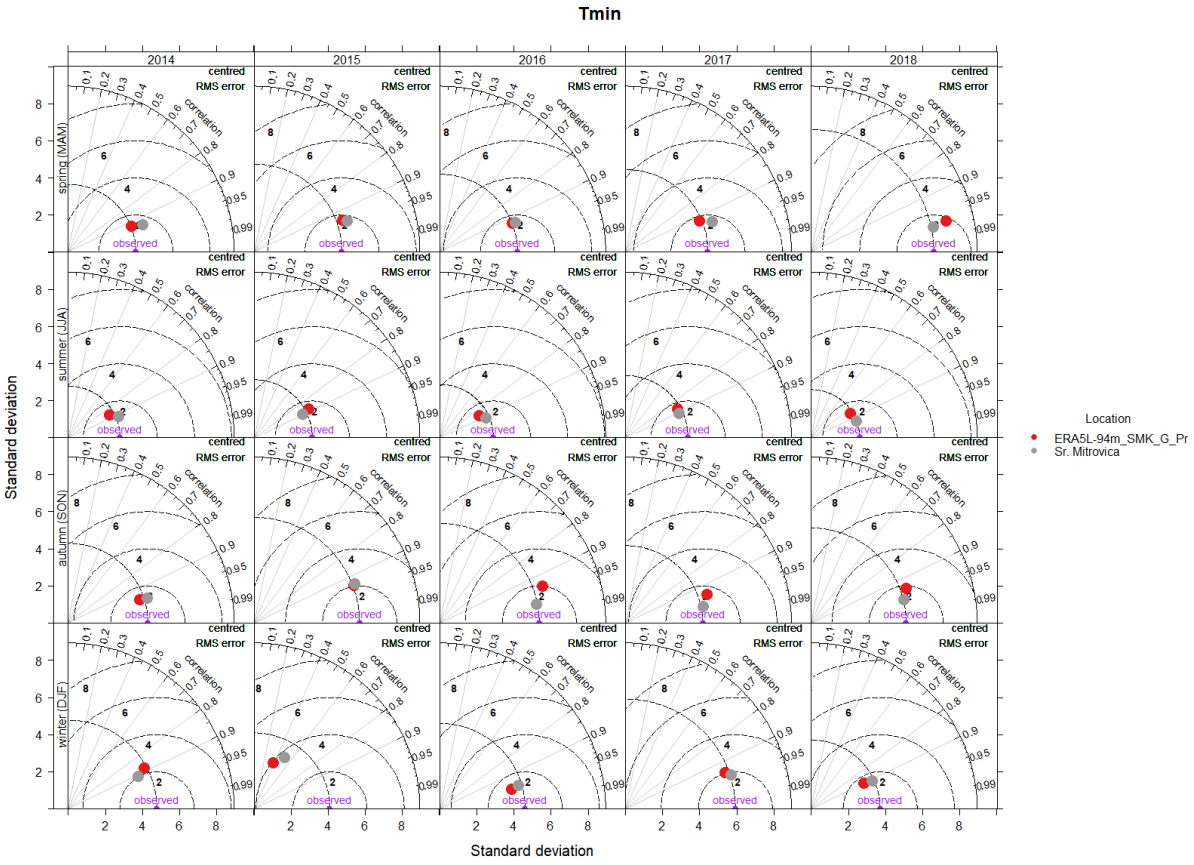


**Figure S5.14** Seasonal Taylor diagram of the $T_{min}$ during the period 2013–2018 observed on 94m_SMK_G_Pr AWS in respect to Sr. Mitrovica climatological station and ERA5-Land reanalysis for the point closest to 94m_SMK_G_Pr.

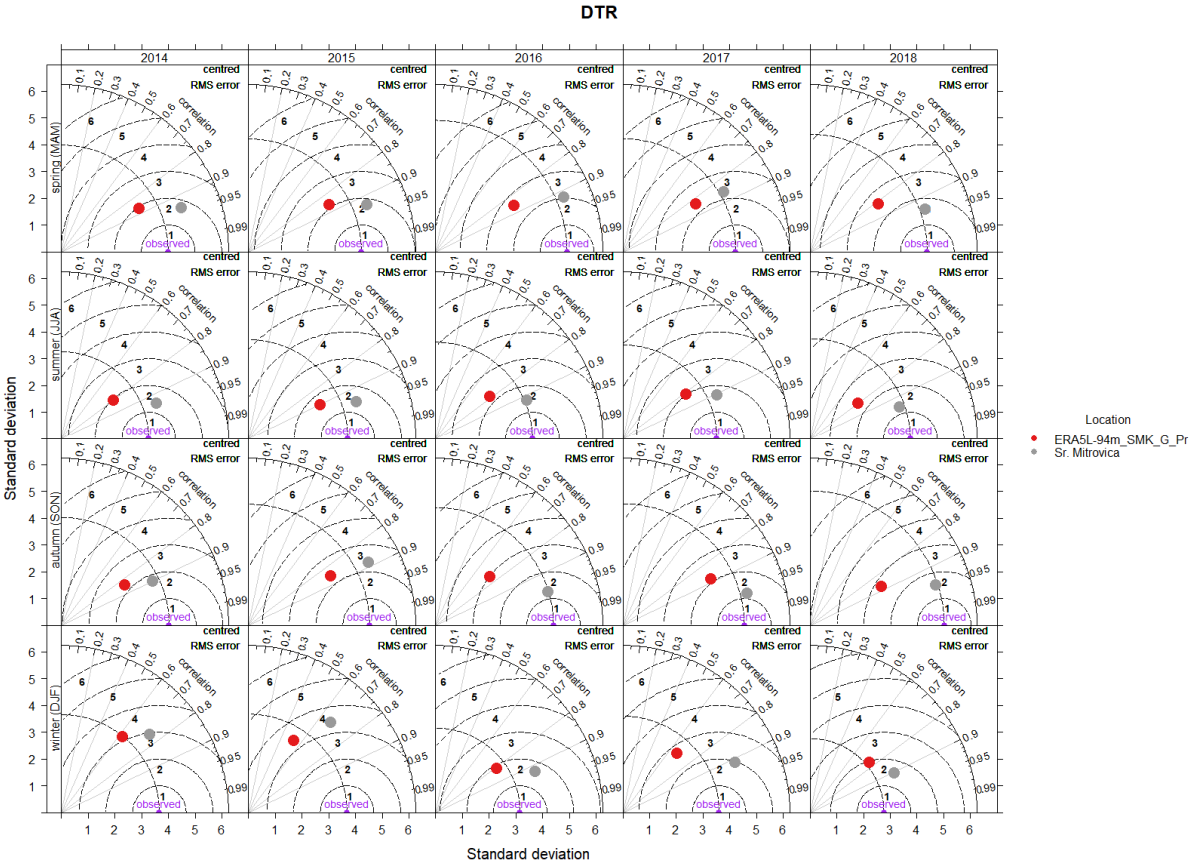

**Figure S5.15** Seasonal Taylor diagram of the DTR during the period 2013–2018 observed on 94m_SMK_G_Pr AWS in respect to Sr. Mitrovica climatological station and ERA5-Land reanalysis for the point closest to 94m_SMK_G_Pr.